**Controlling Polymer Material Structure During Reaction-Induced Phase Transitions** 

Robert J. Hickey\*

Department of Materials Science and Engineering, and Materials Research Institute, The

Pennsylvania State University, University Park, Pennsylvania, 16802, United States

\*Corresponding Author: rjh64@psu.edu

**Abstract** 

Conspectus

Living systems are composed of a select number of biopolymers and minerals yet exhibit an

immense diversity in materials properties. The wide-ranging characteristics, such as enhanced

mechanical properties of skin and bone, or responsive optical properties derived from structural

coloration, are a result of the multiscale, hierarchical structure of the materials. The fields of

materials and polymer chemistry have leveraged equilibrium concepts in an effort to mimic the

structure complex materials seen in nature. However, realizing the remarkable properties in natural

systems requires moving beyond an equilibrium perspective. An alternative method to create

materials with multiscale structures is to approach the issue from a kinetic perspective and utilize

chemical processes to drive phase transitions.

This Account features an active area of research in our group, reaction-induced phase

transitions (RIPT), which uses chemical reactions such as polymerizations to induce structural

changes in soft material systems. Depending on the type of phase transition (e.g., microphase

versus macrophase separation), the resulting change in state will occur at different length scales

(e.g., nm  $-\mu$ m), thus dictating the structure of the material. For example, the in situ formation of

either a block copolymer or a homopolymer initially in a monomer mixture during a

polymerization will drive nanoscale or macroscale transitions, respectively. Specifically, three

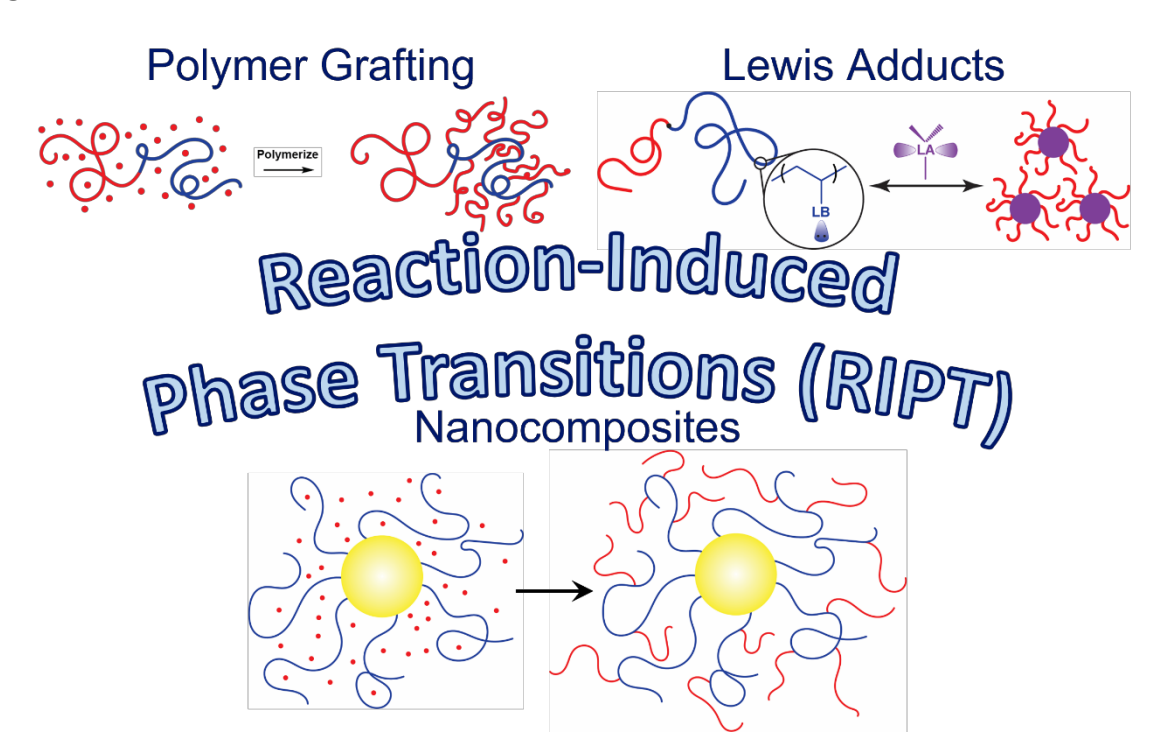
different examples utilizing reaction-driven phase changes will be discussed: 1) in situ polymer

1

grafting from block copolymers, 2) multiscale polymer nanocomposites, and 3) Lewis adduct-driven phase transitions. All three areas highlight how chemical changes via polymerizations or specific chemical binding result in phase transitions that lead to nanostructural and multiscale changes.

Harnessing kinetic chemical processes to promote and control material structure, as opposed to organizing pre-synthesized molecules, polymers, or nanoparticles within a thermodynamic framework, is a growing area of interest. Trapping nonequilibrium states in polymer materials has been primarily focused from a polymer chain conformation viewpoint in which synthesized polymers are subjected to different thermal and processing conditions. The impact of rection kinetics and polymerization rate on final polymer material structure is starting to be recognized as a new way to access different morphologies not available through thermodynamic means. Furthermore, kinetic control of polymer material structure is not specific to polymerizations and encompasses any chemical reaction that induce morphology transitions. Kinetically driven processes to dictate material structure directly impact a broad range of areas including separation membranes, biomolecular condensates, cell mobility, and the self-assembly of polymers and colloids. Advancing polymer material syntheses using kinetic principles such as RIPT opens new possibilities for dictating material structure and properties beyond what is currently available with traditional self-assembly techniques.

TOC



### Introduction

Self-assembly of soft materials has historically been focused on fundamentally understanding equilibrium phase behavior of well-defined components by combining theory and experiment.<sup>1,2</sup> A successful approach in uncovering new morphologies in soft materials involves synthesizing systems with tailored chemical compositions and length scales, and then relating the experimentally determined phase to established theory.<sup>2</sup> Block copolymers, which consist of at least two chemically different polymers covalently attached to form a linear polymer, are a perfect example of how the combination of experiment and theory have led to advances in nanostructured polymer materials (Figures 1a - e).<sup>3</sup> Precision polymerization methods have facilitated the synthesis of block copolymers exhibiting narrow molecular weight distributions, controlled polymer block molecular weights, and volume fractions.<sup>4,5</sup> In parallel with experiments, polymer field theories, computational methods, and molecular simulations have revealed new insights into self-assembled morphologies, demonstrating how the synergistic relationship between theory and experiment has expanded the field (Figures 1a - e). Although thermodynamic approaches have led to important advances and have enabled materials discovery in a host of different applications, recent work highlights how kinetic processing methods reveal new multiscale materials not accessible using traditional polymer blending or self-assembly methods (**Figures 1f – h**).  $^{10,11}$ 

Driving phase changes in materials systems using reaction-induced phase transitions (RIPT),<sup>12</sup> specifically polymerizations, are used commercially in the synthesis of high-impact poly(styrene) (HIPS) and rubber-modified epoxies,<sup>13-15</sup> but has recently led to advances in polymer electrolyte membranes and concentrated colloidal block copolymer solutions.<sup>16,17</sup> RIPT broadly encompasses the use of any chemical reaction, not necessarily polymerization, to drive a phase transition. RIPT examples beyond polymerization include functionalization, deprotection,

conjugations, and chain-scission.<sup>12</sup> Many RIPT examples include polymerizations such as polymerization-induced self-assembly (PISA)<sup>10,18</sup> or polymerization-induced microphase separation (PIMS)<sup>11,19</sup> (**Figure 1f – h**), but there are numerous examples including binding-induced liquid-liquid phase separation in biological systems,<sup>20</sup> degradation/functionalization driven changes in synthetic macromolecular systems,<sup>21,22</sup> or Lewis adduct-induced phase transitions.<sup>23</sup> The phase behavior fundamentals (e.g., macrophase and microphase separation) that control polymer material structure during processing of already synthesized polymers is applicable to chemical reactions,<sup>13</sup> but there is one major difference, the chemical species formed during a reaction are not static and evolve over time. Thus, there are exciting opportunities in applying a broad number of chemical reactions to control material structure while imparting diverse functionality through chemical composition.

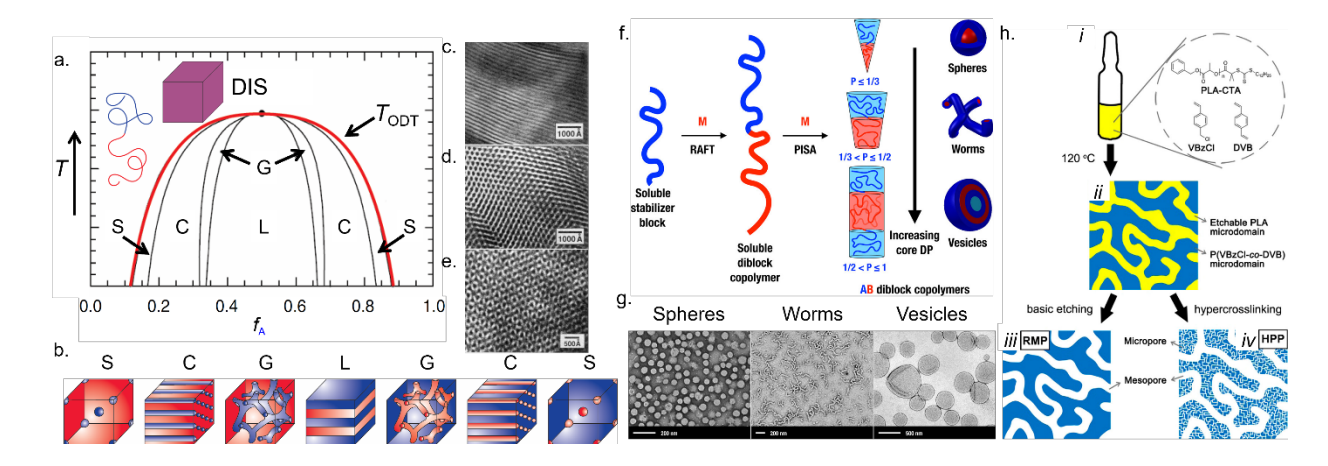


Figure 1. Block copolymer self-assembly using equilibrium and kinetic processes. a) Predicted AB diblock copolymer phase diagram with respect to temperature (T) and volume fraction of block A ( $f_A$ ). The red line represents the boundary between the ordered and disordered phases. Reproduced with permission from reference 8. Copyright 2002 IOP Publishing. b) Schematic representation of prototypical nanoscale morphologies of AB diblock copolymers where S, C, G, and L represent sphere, hexagonally packed cylinder, gyroid, and lamellar morphologies,

respectively. c - e) TEM images of c) L, d) C, and e) G morphologies in a poly(isoprene)poly(styrene) AB diblock copolymers with different volume fractions. Reproduced with permission from reference 5. Copyright 1994 American Chemical Society. f) Scheme showing the polymerization-induced self-assembly (PISA) process in which the polymerization of the second red polymer block from the initial blue polymer block drives the formation of colloidal nanoscale aggregates. The volume fraction of the red block and solvent conditions dictates the polymer chain packing conformation, promoting different nanoscale morphologies. Reproduced with permission from reference 10. Copyright 2016 American Chemical Society. g) TEM images of self-assembled sphere, worm, and vesicle morphologies produced from PISA. Reproduced with permission from reference 10. Copyright 2016 American Chemical Society. h) Example of polymerization-induced microphase separation (PIMS) in which the i) initial poly(lactide) (PLA), styrene, 4-vinylbenzyl chloride (VBzCl), divinylbenzene (DVB) mixture is homogeneously mixed, ii) the onset of phase separation occurs during the polymerization and a trapped co-continuous nanostructure with segregated domains forms at extended polymerization times due to the increase in polymer molecular weight and crosslinking of the poly(styrene) phase. iii) A nanoporous material results on PLA domain removal. iv) A hypercrosslinked structure containing both micro- and mesopores when FeCl<sub>3</sub> is used during the etching process. Reproduced with permission from reference 19. Copyright 2015 American Chemical Society.

Using kinetic self-assembly concepts to create materials is starting to gain momentum and is recognized as a necessary next step in the synthesis of materials with structures not possible within an equilibrium framework.<sup>24</sup> Kinetically driven phase changes open new possibilities to

reach non-equilibrium states, which fall into two general classifications: 1) non-dissipative and 2) dissipative. A non-dissipative non-equilibrium state is one in which the system is kinetically trapped or is in a metastable state. A kinetically trapped system or metastable state is one in which the energy barrier is sufficiently large (e.g., greater than thermal fluctuations, kT) between local and global free energy states. Therefore, kinetically trapped systems are "stuck" in the resulting state until external influences (e.g., thermal) push the system over the energy barrier to transition to a preferred state. A dissipative non-equilibrium state occurs when a constant energy input is supplied to the system to maintain the desired state. Living systems are prime examples of how dissipative non-equilibrium processes in cells enable daily function. Biological organisms produce energy through a series of chemical reaction networks that sustain homeostasis. If the energy source is stopped, the system will eventually transition into an equilibrium state.

In polymer systems, non-dissipative non-equilibrium structures are common and typically form during processing.  $^{26,27}$  From a general standpoint, if a polymer melt is deformed during processing on a timescale that is faster than the longest relaxation of the chain, the polymer chain will adopt a non-equilibrium conformation.  $^{26}$  The deformed polymer sample will be trapped in the non-equilibrium state if it is thermally quenched below the glass transition temperature ( $T_g$ ) or the crystallization temperature ( $T_g$ ) at a rate faster than the chain can relax.  $^{26}$  Flow-induced crystallizing during injection molding is a commercially relevant example that results in a trapped non-equilibrium polymer chain conformation due to processing and then crystallization (i.e., rapid cooling), directly impacting material structure and properties.  $^{28}$ 

Porous polymer membranes produced using non-solvent-induced phase separation (NIPS) result in non-dissipative non-equilibrium structures that are produced by kinetically trapping polymer phase separation in a non-solvent triggered by solvent exchange.<sup>27</sup> In the case of

homopolymers in an initially good solvent, kinetically trapping of the macrophase separated state occurs when the polymer either vitrifies or crystallizes at a specific time point during solvent/non-solvent exchange.<sup>27</sup> The point at which the polymer is trapped corresponds to a specific polymer/good solvent/poor solvent composition within a ternary phase diagram.<sup>27</sup> Similar to solvent exchange, quick solvent evaporation of a block copolymer/additive blend, inducing spinodal decomposition of the mixture, results in hierarchically ordered materials.<sup>29</sup> Analogous NIPS methods have been used to create hierarchical hydrogels that demonstrate enhanced elongation and softness,<sup>30</sup> which is drastically different from hydrogels composed of the same polymer but produced using equilibrium techniques.

The literature related to non-equilibrium self-assembly in polymer systems is primarily focused on post-polymerization processing such as flow or shear induced crystallization, or spin-coated polymer films. <sup>26</sup> There is significant room for growth from an experimental and theoretical perspective with respect to controlling polymer material structure from a kinetic standpoint during a chemical reaction. Here, the Account will focus on three areas in which RIPT has been used in our group to control polymer material structure. The first part will describe how polymer grafting from well-defined block copolymers induces nanostructural changes and is adaptable to a commercial thermoplastic elastomer, resulting in enhanced mechanical properties. New approaches to synthesize polymer nanocomposites with controlled nanoparticle organization at multiple length scales are highlighted in the second example. The last example demonstrates how Lewis adduct formation in polymer systems induces either macrophase or nanoscale phase transitions in homopolymer and block copolymer systems, respectively. Finally, the Account will end with an outlook detailing future directions regarding the use of chemical reactions to drive material structure and property.

# In Situ Polymer Grafting from Block Copolymers

Polymerization-induced phase changes have primarily focused on growing a second polymer block from a homopolymer to form a linear diblock copolymer that will self-assemble into nanoscale morphologies due to the second block incompatibility in the reaction mixture (**Figures 1f**, **g**). <sup>10</sup> A prime example is PISA, pioneered by Armes and co-workers, which is conducted in solution where the monomer used to form the second block is miscible in the solvent, but as the degree of polymerization (*N*) reaches a critical value, the block phase separates at the nanoscale forming a high concentration of colloidal aggregates (**Figures 1f**, **g**). <sup>10,18</sup> To date, numerous polymerization methods have been reported and recent work has broadened the field to incorporate new stimuli such as light to initiate the polymerization or have moved beyond linear chains to grafted copolymers and supramolecular polymerizations. <sup>17,31</sup> Furthermore, the industrial potential for using PISA to synthesize nanoscale colloidal aggregates is starting to be realized via high-throughput synthesizers and continuous flow reactors. <sup>17</sup>

Hillmyer and co-workers have shown that diblock copolymer synthesis in the bulk using liquid monomer with crosslinker will lead to the formation of co-continuous materials by kinetically trapping the microphase separated, but disordered, morphology before ordering (**Figure 1h**). In a typical reaction, a homopolymer end functionalized with a chain transfer reagent (macro-CTA) is blended with liquid monomer and crosslinker, and then polymerized. During the polymerization, the second polymer block grows in addition to being crosslinked. As the molecular weight of the second polymer block increases, the system will begin to microphase separate, but the transition to an ordered mesophase is prevented due to crosslinking, trapping the co-continuous morphology. Removal of one polymer block results in a nanoporous material.

Recently, our group has shown that polymer grafting from one block of a diblock copolymer, forming a linear-comb copolymer, during polymerization will induce nanostructural transitions (**Figure 2a**).<sup>32-34</sup> The first report from the group showed that either lamellar-to-hexagonally packed cylinder (L-to-C) or disordered-to-hexagonally packed cylinder (DIS-to-C) morphology transitions are possible using poly(styrene)-poly(1,2-butadiene) (PS-PBD) as the diblock copolymer and styrene as the monomer (**Figure 2b**).<sup>32</sup> The polymerizations are conducted by first blending the PS-PBD with styrene, a radical initiator, and 4-hydroxy-2,2,6,6-tetramethylpiperdine 1-oxyl (4-hydroxy-TEMPO), heating to 125 °C, conducting the polymerization for 3 h, and then cooling to room temperature. The choice of the radical initiator is critical.<sup>32</sup> Here, benzoyl peroxide (BPO) will abstract a hydrogen from a carbon that is adjacent to the vinyl group (i.e., allylic hydrogen), resulting in the formation of a radical that will initiate the polymerization of PS from the PBD backbone.<sup>32</sup> Furthermore, 4-hydroxy-TEMPO controls the propagation of the PS chains.

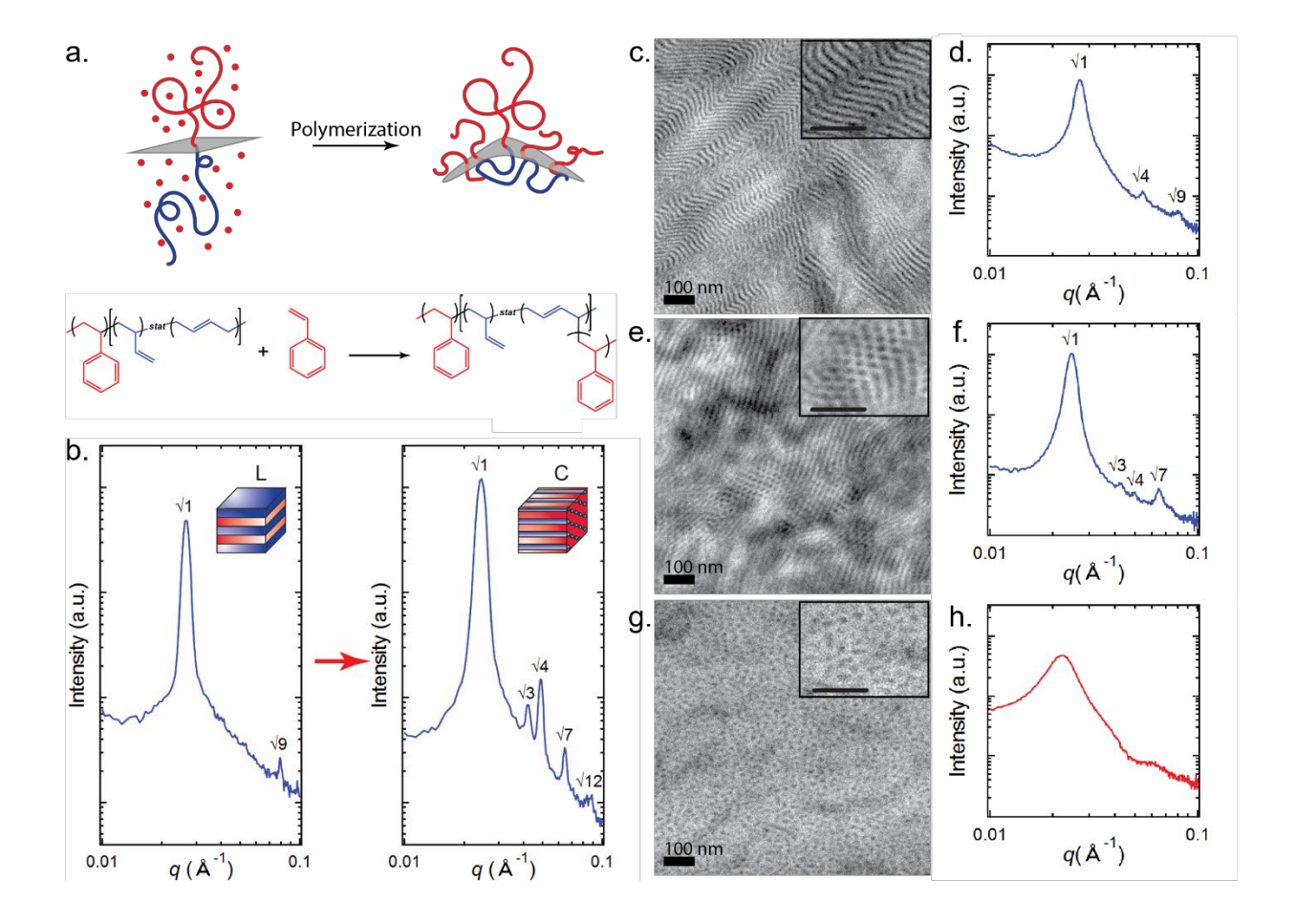


Figure 2. In situ polymer grafting from an AB diblock copolymer, drives nanoscale morphology changes. a) PS grafting from the PBD block of a PS-PBD diblock copolymer occurs via the formation of allylic radicals. The synthesis of a linear-comb block copolymer promotes the transition to a different nanoscale morphology. b) Room temperature SAXS plots indicate a nanoscale morphology change from the initial lamellar (L) morphology to the hexagonally-packed cylinder (C) morphology before and after polymerization, respectively. c - h TEM images and corresponding SAXS plots for c, d L, e, f C, and g, h disordered sphere phases after

polymerization. The different morphologies are produced by changing the initial PS-PBD/styrene volume fraction where the formation of disordered spheres form at the highest styrene amount. Scale bars for inset TEM images are 100 nm. Reproduced with permission from reference 32. Copyright 2018 American Chemical Society.

The morphology of the PS-PBD system measured by small-angle X-ray scattering (SAXS) at room temperature are drastically different before and after polymerization (**Figure 2b**).<sup>32</sup> PS grafting from the PBD block, initiated by the formation of an allylic radical on the PBD block, affords the poly(styrene)-block-[poly(butadiene)-graft-poly(styrene)] (PS-PBD-g-PS) linear-comb copolymer. PS grafting from the PBD block is essential in the polymerization-induced DIS-to-C transition because simply blending PS homopolymer with the PS-PBD diblock at the same volume fraction results in a microemulsion, not an ordered nanoscale morphology.<sup>32</sup> A variety of nanoscale phases are achievable after the polymerization, as confirmed using transmission electron microscopy (TEM) and SAXS (**Figures 2c - h**),<sup>32</sup> through the allylic grafting procedure by changing the initial PS-PBD/styrene volume fraction.

The L-to-C order-to-order transition (OOT) induced by the formation of polymer grafts from the PBD block shown in **Figure 2b** exhibits a complex self-assembly mechanism that is atypical of standard OOTs seen in linear diblock copolymer systems (**Figure 3a**). The transition between ordered L, C, and gyroid (G) morphologies in linear AB diblock copolymers (e.g., G-to-C or L-to-G) proceeds through a nucleation and growth process in which the new phase first forms a stable nucleus and then grows epitaxially along preferred crystallographic orientations due to the required matching between the domain spacings of the two phases. In the L-to-C OOT driven by polymerization (**Figure 3a**), the L phase first disorders at elevated temperature (e.g., 125 °C), and

then re-orders over time during the polymerization (**Figure 3a**). The transition from DIS-to-order during the polymerization suggests that N of the block copolymer is increasing, supporting the proposed polymer grafting mechanism.

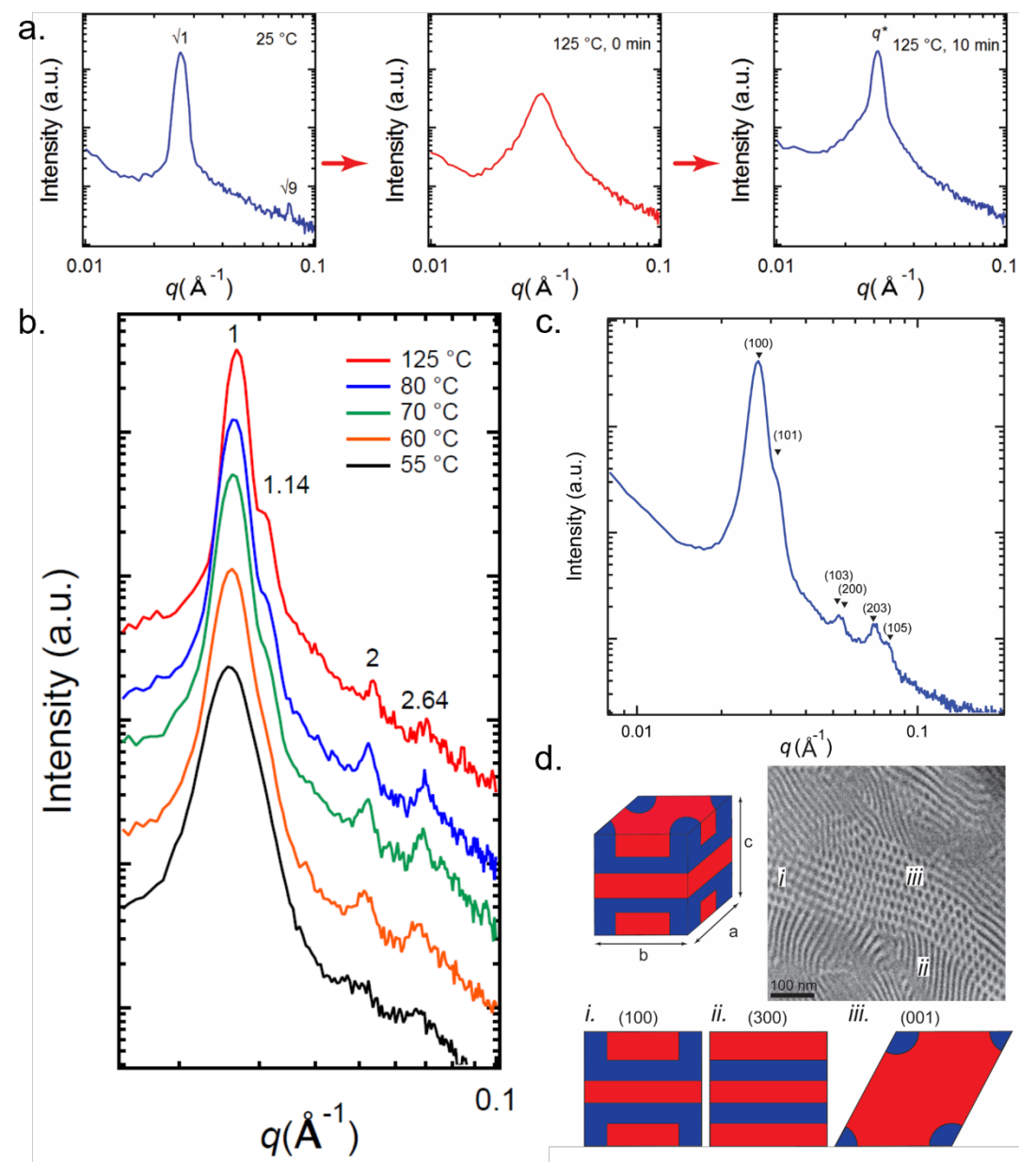


**Figure 3. Tracking the nanoscale morphology transition during polymerization.** a) SAXS plots showing that the lamellar morphology of the initial PS-PBD/styrene mixture at 25 °C first disorders when heated to 125 °C and then orders after 10 min due to the polymerization process. b) The high temperature morphology after 3 h of polymerization transitions to a C phase when the

temperature if cooled to 55 °C. c) Room temperature SAXS plot of the polymerized sample after 21 h. The extended polymerization time traps the high temperature morphology. d) TEM image of the high temperature HPL phase with corresponding unit cell and *i*) (100), *ii*) (300), and *iii*) (001) Miller planes. Reproduced with permission from reference 33. Copyright 2020 American Chemical Society.

On completion of the polymerization, the new phase that forms at elevated temperature (e.g., 125 °C) is distinctly different from the initial L phase at room temperature before polymerization (**Figure 3b**). Interestingly, the high temperature nanoscale phase after polymerization is found to be a hexagonally perforated lamellae (HPL) phase, which is supported by the SAXS pattern and TEM images (**Figures 3c, d**).<sup>33</sup> When the polymerized sample is cooled to 55 °C after the 3 h polymerization, the HPL phase transitions to C (**Figure 3b**). In order to elucidate the high temperature phase at room temperature as shown in **Figures 3c** and **d**, the polymerization was conducted for 21 h to kinetically trap the HPL phase through a combination of crosslinking and an increase in the glass transition temperature.

The formation of the HPL phase after polymerization and the thermoreversible morphology transition between HEX on cooling and heating suggests that the HPL phase in the PS-PBD-g-PS copolymer system is thermodynamically stable. The HPL phase in linear AB diblock copolymers is a metastable transition state between G-to-C and L-to-G.<sup>38</sup> It is predicted that there is a significant nucleation barrier associated with the L-to-G transition, and the HPL phase is the kinetically favored intermediate state.<sup>38</sup> In grafted or miktoarm star copolymer systems, the perforated lamellae morphology demonstrates increased stability as compared to the AB diblock

copolymer systems,<sup>39</sup> which is consistent with self-consistent field theory results for star and comb copolymers exhibiting high compositional asymmetries.<sup>40</sup>

The same polymer grafting chemistry using allylic radicals is adaptable to block copolymers with different macromolecular architectures such as ABA triblock copolymers.<sup>34</sup> Specifically, when a prototypical thermoplastic elastomer, poly(styrene)-poly(butadiene)-poly(styrene) (SBS) triblock copolymer, is blended with styrene monomer and BPO, and polymerized at 100 °C for 3 h, the initial disordered sphere morphology transitions to L (**Figures 4a – c**). Similar to the PS-PBD diblock copolymer example discussed above, allylic radicals are generated on the PBD-block and initiate the polymerization of styrene forming PS grafts. The increase in the PS volume fraction is predicted to drive the morphology transition as shown in the SAXS plots (**Figure 4d**). Changing the initial SBS/styrene volume fraction ( $\varphi_{SBS}$ ) results in the formation of a L morphology over a large compositional window (e.g.,  $\varphi_{SBS} \approx 50 - 20\%$ ) and finally ending with co-existing phases when  $\varphi_{SBS} = 10\%$ .

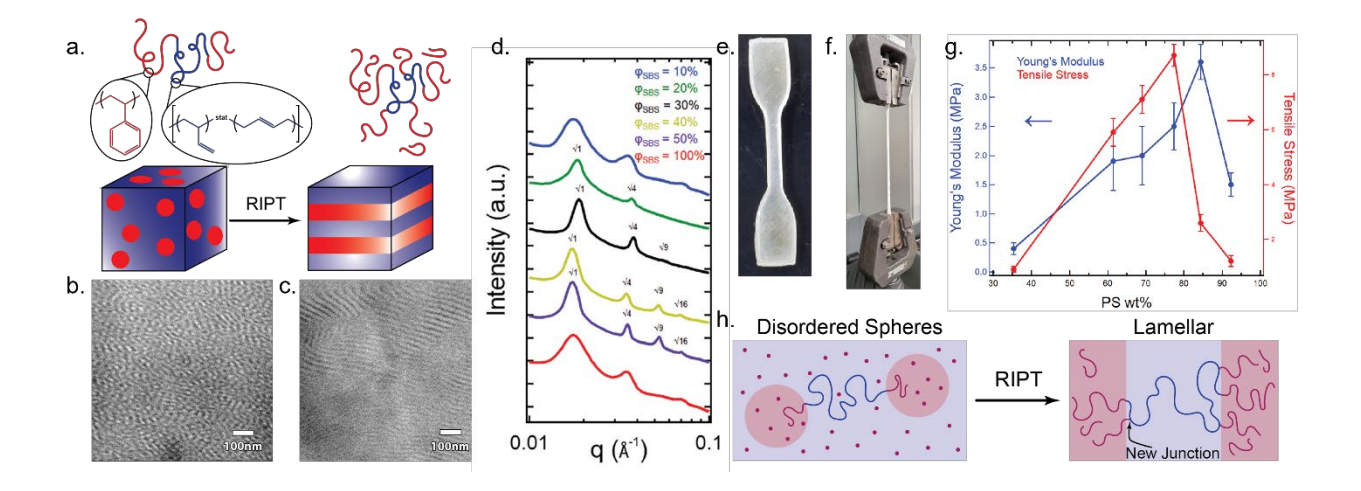


Figure 4. Polymer grafting from the PBD mid-block of SBS leads to nanostructural transitions and enhances the mechanical properties. a) A scheme depicting the polymerization-induced transition from disordered spheres to a lamellar morphology, which is driven by PS

grafting from the mid PBD block. TEM images of the b) disordered sphere and c) L morphologies before and after polymerization, respectively. d) Room temperature SAXS plots after polymerization indicate a change in nanoscale morphology with increasing styrene content. Assigned nanoscale morphologies for the SAXS plots are reported as disordered spheres, lamellar, and a co-existing microphase for  $\phi_{SBS} = 100\%$ ,  $\phi_{SBS} = 50 - 20\%$ , and  $\phi_{SBS} = 10\%$ , respectively. Photographs of the e) dog bone sample prepared from conducting the polymerization in a silicone mold and f) uniaxial extension tensile measurement to determine the mechanical properties of the polymer samples. g) A plot showing the change in Young's modulus and tensile strength of the polymer samples with respect to PS wt%. h) Proposed polymer chain orientation in the polymer samples before and after polymerization. PS grafting from the mid PBD block is expected to increase the number of junctions in the L morphology, enhancing the mechanical properties. Reproduced with permission from reference 34. Copyright 2021 Royal Society of Chemistry.

The SBS/styrene blending protocol affords the opportunity to synthesize nanostructured materials in a mold, which is important for creating samples for mechanical testing (**Figures 4e**, **f**).<sup>34</sup> A series of molded dog bone samples were prepared at different φ<sub>SBS</sub> and tested using uniaxial extension to determine stress-strain curves. From the stress-strain curves, the Young's modulus and tensile strength were determined for each sample and plotted in **Figure 4g**. As shown in **Figure 4g**, the changes in Young's modulus and tensile strength are non-monotonic with respect to PS wt%. Young's modulus and tensile strength increase with PS content, reach a maximum, and then rapidly decrease. The initial increase in Young's modulus and tensile strength with increasing PS content is predicted to be a result of two variables: 1) the addition of high modulus PS will increase the Young's modulus due to the rule of mixtures and 2) grafting from the PBD block will enhance

the physical crosslinking.<sup>41</sup> The relative impact between PS content and number of polymer grafts is being actively explored by precisely controlling polymer grafting to reveal the relationship between macromolecular architecture and nanostructure.

# **Multiscale Polymer Nanocomposites**

Polymer nanocomposites are hybrid materials containing polymers and inorganic nanoparticles and are used in a number of commercial applications such as filled rubbers and reinforced thermosets.<sup>42</sup> There are numerous methods for preparing polymer nanocomposites, but the field has been primarily focused on blending nanoparticles and polymers. 43 There are major enthalpic and entropic mixing energy barriers associated with blending nanoparticles and polymers, hindering precise control over nanoparticle organization and thus material property.<sup>43</sup> An alternative approach to synthesizing nanocomposites that has gained renewed attention is polymerizing nanoparticle/monomer mixtures to kinetically trap the initially dispersed nanoparticles in the polymer matrix. The utility of synthesizing polymer nanocomposites via polymerizing monomer in the presence of nanoparticles was first reported in two 1993 Toyota articles reporting that the synthesized polymer nanocomposite materials exhibit increases in mechanical and heat deflection temperature properties compared to the neat polymer materials, reinvigorating the nanocomposite field. 44,45 Although the enhanced material properties sparked excitement in the field, the synthetic approach was in a way overlooked, especially regarding nanoparticle distribution within the polymer matrix.

The major benefit of polymerizing nanoparticle/monomer mixtures over standard blending procedures is that the free energy of mixing is significantly reduced due to maximizing the entropy of mixing as  $N \rightarrow 1$ . Therefore, with the right nanoparticle surface functionalization and/or reaction

mixture composition (i.e., minimizing the enthalpic penalty), many nanoparticles will disperse within the monomer reaction mixture.<sup>46</sup> Numerous different nanoparticles such as carbon,<sup>47,48</sup> SiO<sub>2</sub>,<sup>49,50</sup> TiO<sub>2</sub>,<sup>46</sup> ZnO,<sup>46</sup> ZrO<sub>2</sub>,<sup>46</sup> and Au<sup>51</sup> have been incorporated within polymer matrices through the described polymerization method, but most of the reports have focused on synthesizing the materials without exploring how the polymerization impacted nanoparticle distribution.

To address the impact of nanoparticle organization in a polymer matrix during polymerization, we adapted the allylic radical initiated polymer grafting chemistry described in the In Situ Polymer Grafting from Block Copolymers section above to polymer grafted nanoparticles (PGNs) (Figure 5).<sup>49</sup> Poly(cyclooctadiene) (PCOD) grafted silica nanoparticles were prepared using surface-initiated ring-opening metathesis polymerization (SI-ROMP)<sup>52</sup> resulting in PCOD grafts with a weight-average molecular weight  $(M_w)$ , dispersity (D), and polymer graft density ( $\sigma$ ) of 13 kg/mol, 1.51, and 0.03 chains/nm<sup>2</sup>, respectively. PCOD is structurally similar to 1,4PBD and was found to initiate the polymerization of polymer grafts via allylic radicals (Figure 5b). The polymer grafting from PCOD was confirmed using a combination of dynamic light scattering (DLS) and molecular weight characterization for the polymer chains cleaved from the nanoparticle surface.<sup>49</sup> Thus, by blending PCOD PGNs with styrene and BPO, and conducting the polymerization, polymer nanocomposites with dispersed PGNS were formed (Figure 5c). The polymerization method was adapted to synthesize nanocomposites containing poly(methyl methacrylate) (PMMA) by replacing styrene with methyl methacrylate in the initial reaction mixture. Furthermore, the polymerization procedure enables large batches of material to be produced that are easily processable without leading to changes in nanoparticle dispersion, as confirmed by TEM before and after processing (Figure 5d).

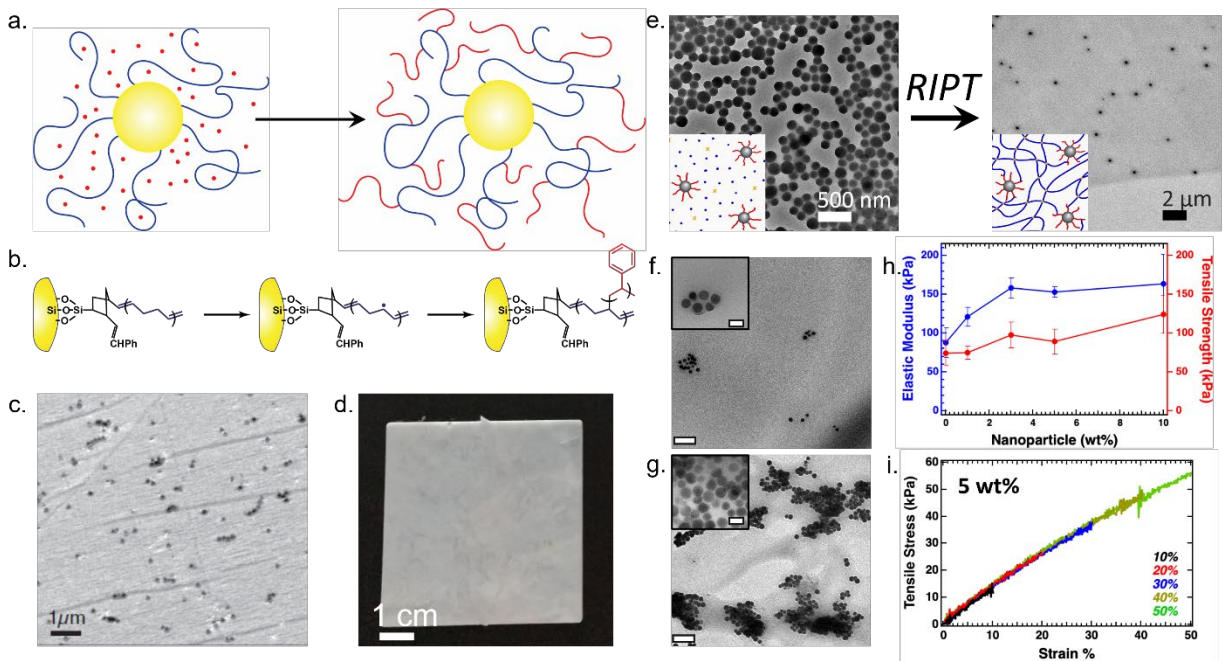


Figure 5. In situ polymer grafting from polymer grafted nanoparticles promotes nanoparticle dispersion and enhances the mechanical properties. a) Scheme illustrating the polymer grafting process from polymer grafted nanoparticles. b) Allylic radical initiated polymerization to form PS grafts from PCOD chains that are attached to a nanoparticle surface. c) TEM image of a polymer nanocomposite containing 5 wt% PCOD PGNs in polymer styrene. d) Photograph of polymer nanocomposite film that was prepared by thermally pressing PCOD PGNs/PS sample containing 5 wt% nanoparticle after polymerization. Reproduced with permission from reference 49. Copyright 2020 AIP Publishing. e) TEM images before and after polymerization of PNBE PGNs initially dispersed in a mixture containing lauryl methacrylate, crosslinker, and BPO. TEM images of polymer nanocomposites containing f) 1 wt% and g) 10 wt% PNBE PGNs. h) Plot showing changes in elastic modulus and tensile strength of the polymer nanocomposites with increasing nanoparticle loading while at constant crosslink density. i) Reversible deformation of prepared polymer nanocomposites containing 5 wt% PNBE PGNs

showing minimal to no hysteresis up to 50% strain. Reproduced with permission from reference 50. Copyright 2022 Elsevier.

The dispersion state of the PCOD PGNs in PS or PMMA matrices is predicted to be dependent on the ability to graft PS and PMMA from PCOD, respectively, via allylic radicals. For example, grafting PS chains from PCOD will reduce the enthalpic mixing barrier relative to the PS/PCOD interaction, promoting dispersion. Furthermore, the grafted PS chains will help to prevent nanoparticle aggregation. Related grafting procedures are used in the production of high-impact poly(styrene) (HIPS) and acrylonitrile-butadiene-styrene (ABS) where poly(butadiene) homopolymer is initially blended with either styrene or styrene/acrylonitrile monomers, respectively.<sup>53</sup> During the polymerization of the monomers, rubber particles composed of poly(butadiene) form and are stabilized in either PS or poly(styrene-co-acrylonitrile) (SAN) matrices due to polymer grafting from the PBD particles.<sup>15,53</sup> Polymer grafts from PBD are predicted to result from allylic radials that form during the polymerization process. Without polymer grafting, the PBD phase would macrophase separate into two distinct phases.

Our group recently adapted the allylic radical polymer grafting procedure initially used to form amorphous, glassy polymer nanocomposites to synthesize soft hybrid elastomers (**Figure 5e**). In the reported article, poly(norbornene) (PNBE) grafted silica nanoparticles were prepared using SI-ROMP, similarly to the PCOD PGNs, and blended with lauryl methacrylate, crosslinker, and BPO (**Figure 5e**). The PNBE PGNs become trapped in the crosslinked polymer matrix during the progression of the polymerization. A series of nanoparticle loadings ranging from 0 - 10 wt% with respect to the polymer matrix were prepared and characterized structurally and mechanically. In all cases, discrete nanoparticle aggregates form and increase in size with nanoparticle loading

(Figures 5f, g). The crosslinked polymer matrix is predicted to prevent macrophase separation, which is predicted from the composite morphology diagram plotted as the product of the polymer grafting density and square root of the polymer graft degree of polymerization ( $\sigma \sqrt{N}$ ) versus the ratio of the polymer matrix and polymer graft degrees of polymerization (P/N). Crosslinking will drastically increase the polymer matrix degree of polymerization. Mechanical analysis using uniaxial extension reveals that the elastic modulus and tensile strength of the polymer nanocomposites increase with nanoparticle loading while at constant crosslink density (**Figure 5h**). Furthermore, the polymer nanocomposites demonstrate reversible deformation up to 50% strain with minimal to no hysteresis (**Figure 5i**).

The previous two examples highlight how the RIPT process effectively disperses nanoparticles in glassy and elastomeric polymer matrices through grafting polymers from PGNs. Alternatively, it is possible to synthesize polymer nanocomposites with multiscale structures by inducing macrophase separation and nanoparticle aggregation in a two-step process during polymerization (**Figure 6**).<sup>51</sup> Gold nanoparticles (AuNPs) functionalized with oleylamine were first synthesized in a methyl methacrylate (MMA) solution (**Figures 6a, b**), which was adapted from a previous method using toluene as the solvent.<sup>55</sup> The AuNP/MMA solution is dark red, similar in appearance to AuNPs produced using toluene as the solvent (**Figure 6b**).<sup>55</sup> The AuNP/MMA solution is then diluted further with MMA for desired MMA volume fractions ( $\Phi_{MMA} = 90, 85, 80, \text{ and } 75\%$ ).

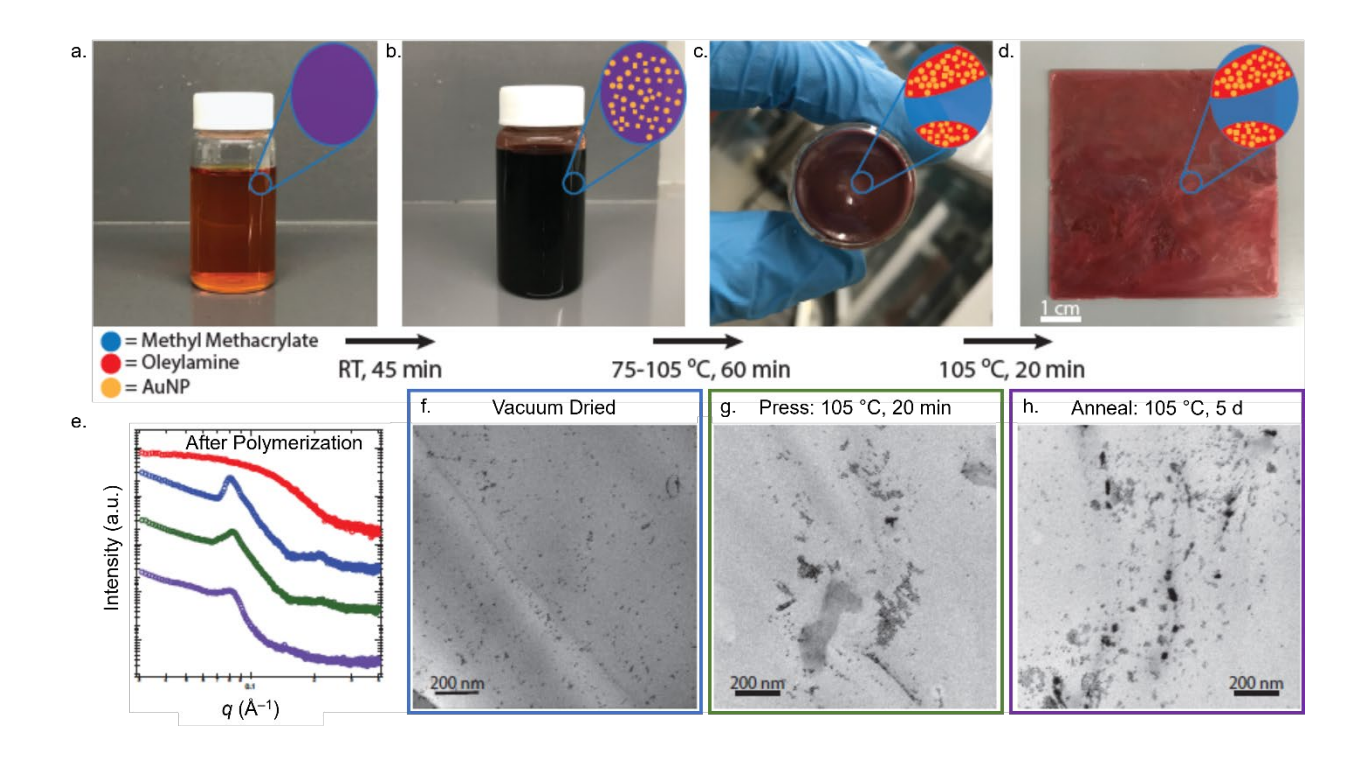


Figure 6. Synthesis of multiscale polymer nanocomposites using a two-step self-assembly procedure during polymerization and processing. a) AuNPs were synthesized by first mixing gold precursors in a methyl methacrylate solution and then b) adding reducing agent to form the nanoparticles. The AuNP/MMA mixture was further diluted with additional MMA to reach the desired MMA volume fraction and then c) polymerized at different temperatures for 60 min, and d) finally vacuum drying to remove unreacted monomer and thermally pressing to form a polymer nanocomposite film. e) Room temperature SAXS plots and f - h) TEM images of the AuNP/PMMA material directly after polymerization (red SAXS curve), f) vacuum drying (blue SAXS curve), g) thermally pressing (green SAXS curve), and h) annealing at 105 °C (purple SAXS

curve). Reproduced with permission from reference 51. Copyright 2021 American Chemical Society.

All samples prepared at different  $\Phi_{MMA}$  resulted in solid materials after polymerization (Figure 6c). The materials after polymerization were further processed by first removing unreacted monomer via vacuum drying and then thermally pressing into square geometries for characterization. The initial AuNP/MMA solutions were homogeneous, but upon polymerization forming PMMA, the system macrophase separates, forming oleylamine- and PMMA-rich domains. Interestingly, although the system is macrophase separated after polymerization, the AuNPs appear homogeneously mixed as indicated from the SAXS plot shown in Figure 6e. Typically, aggregated nanoparticle materials exhibit an interparticle correlation peak corresponding to the nanoparticle center-to-center distance in a SAXS plot, which is not present directly after polymerization (Figure 6e, red curve). The interparticle correlation peak does appear after vacuum drying and remains at constant scattering vector, q, when the samples are thermally pressed and annealed (Figure 6e, blue, green, and purple curves). TEM images of samples after vacuum drying (Figure 6f), thermally pressing (Figure 6g), and annealing (Figure 6h) imply that the AuNP aggregates increase in size during the processing steps. Thus, the two-step phase separation process first involves macrophase separation forming oleylamine- and PMMA-rich domains that are expected to be on the order of micrometers, and then finally nanoscale AuNP aggregation, resulting in multiscale structured materials. Separating the two-phase separation processes permits one to independently control the self-assembly process; potentially leading to multiscale structures in which nanoparticles organize into well-defined nanostructures by tuning interparticle interactions.

### **Lewis Adduct-Driven Phase Transitions**

The previous two sections emphasized how polymerizations drive block copolymer and nanoparticle self-assembly under kinetic conditions. As stated earlier, RIPT broadly defines how any chemical reaction drives a phase change, which is nicely demonstrated via polymerizations, but RIPT is more encompassing. For example, binding-induced liquid-liquid phase separation is ubiquitous in biological and synthetic macromolecular systems and is triggered either by the formation of protein-ribonucleic acid (RNA) complexes or complex coacervation, respectively. The phase separation process in these examples is attributed to changes in entropy, which is due to the increase in the "degree of polymerization" of the complexes with respect to extent of binding. Although entropy is important for such systems, non-covalent association can cause changes in electronic structure, leading to changes in enthalpic interactions such as those driven by dipole associations or  $\pi - \pi$  stacking. Thus, it is critical to determine the interplay between enthalpic and entropic changes due to supramolecular association and phase separation to predict phase transitions in associating systems.

Recently, our group revealed that Lewis acid/base adduct formation between a poly(Lewis base) and a Lewis acid will induce either macrophase or nanoscale phase transitions (**Figure 7**).<sup>23</sup> In the case of macrophase separation, when poly(diphenylphosphinostyrene) (PDPPS) in toluene is mixed with tris(pentafluorophenyl)borane (BCF) that is also initially dissolved in toluene, the solution will macrophase separate when the boron to phosphorous mole ratio (B/P) is greater than 0.2 (**Figure 7a**). The Lewis adduct-induced macrophase separation is predicted to result from the strong B-P bond, which would give rise a negative interaction parameter ( $\chi$ ). The experimental results were further supported by establishing a predicted phase diagram using a modified Flory-

Huggins model for a ternary mixture containing PDPPS, BCF, and toluene.<sup>23</sup> There is excellent agreement between the experimental results and the predicted ternary phase diagram, indicating that strong intermolecular interactions have the potential to drive phase changes.

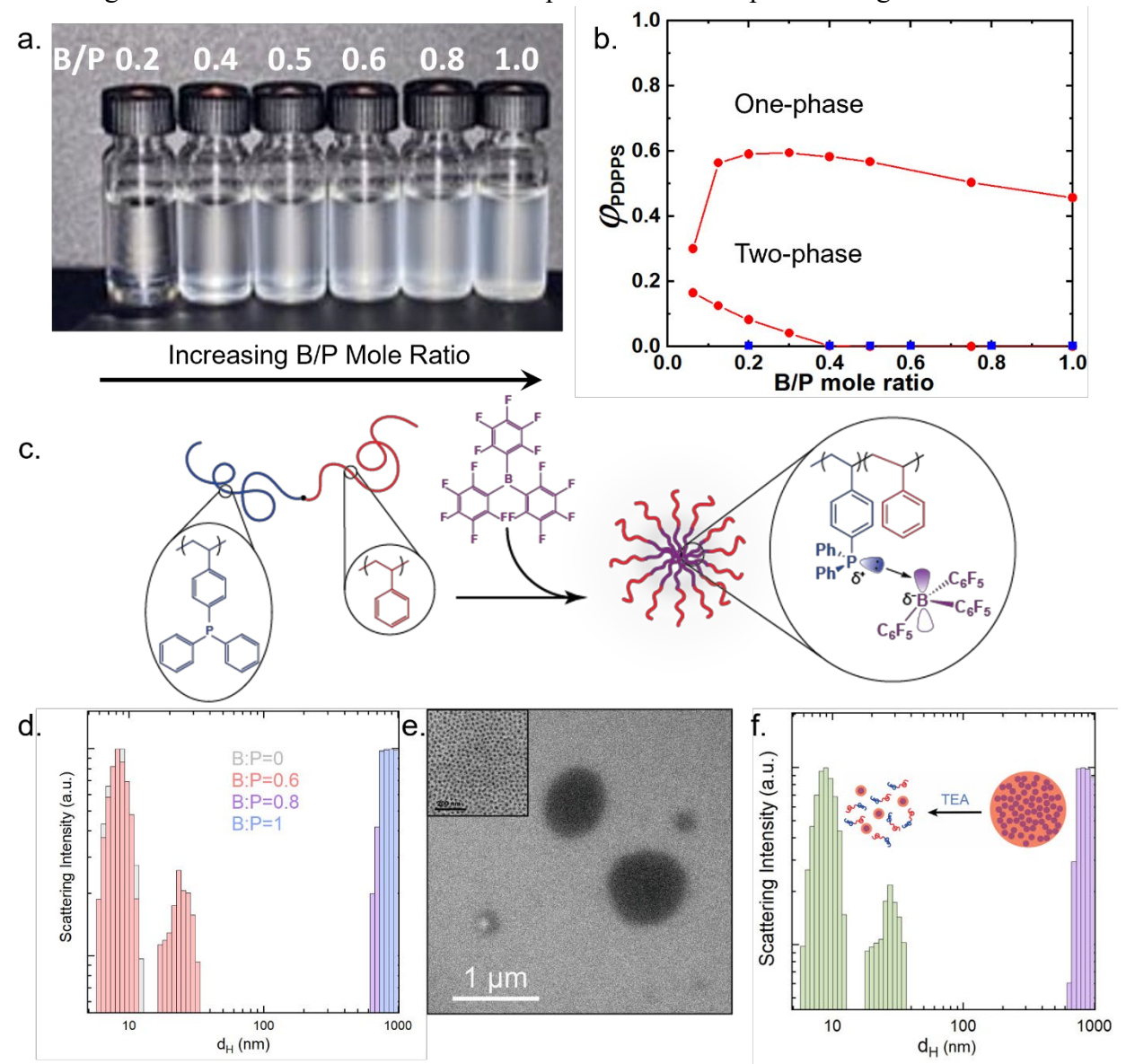


Figure 7. Lewis adduct-induced macrophase and nanoscale separation. a) Photographs showing macrophase separation in PDPPS/BCF/toluene mixtures when the B/P mole ratio is increased from 0.2 to 1. b) Phase diagram plotted as volume fraction of PDPPS in toluene versus B/P mole ratio. The red line is the predicted binodal line separating one-phase and two-phase regions. The blue data points are experimentally established from visually inspecting the ternary

mixtures shown in **Figure 7a**. Although the blue data points appear to be on the x-axis, the PDPPS volume fraction is not zero. c) Scheme showing the Lewis adduct-induced micellization process when BCF is added to a PS-PDPPS solution. The formation of the Lewis adduct will form a dipole, which is expected to change the interaction parameter between the polymer and solvent. d) DLS plot showing an increase in the colloidal aggregate size with increasing B/P mole ratio when BCF is added to a PS-PDPPS/toluene mixture. e) TEM image showing the formation of large nanostructured colloidal aggregate prepared from a PS-PDPPS/BCF sample with a B/P = 0.8 mole ratio. The inset image shows the nanoscale micelles. The scale bar is 200 nm. f) DLS plot showing the reversible micellization process when a stronger Lew base (e.g., triethylamine (TEA)) is added to the PS-PDPPS/BCF mixture. The large colloidal aggregates transition to isolated micelles and PS-PDPPS diblock copolymer chains. Reproduced with permission from reference 23. Copyright 2022 American Chemical Society.

The existence of a two-phase region, as shown in **Figure 7b** for the PDPPS/BCF/toluene mixture, implies that a block polymer containing a non-interacting polymer (e.g., PS) and PDPPS will also lead to the self-assembly of colloidal nanostructures on adduct formation (**Figure 7c**). A toluene solution containing PS-PDPPS undergoes a micellization process when BCF is added to the solution. The dynamic light scattering (DLS) data shown in **Figure 7d** indicates there is an increase in the hydrodynamic diameter ( $d_H$ ) from 8.3 nm to 22.1 when B/P = 0.6. Increasing the B/P ratio further (e.g., B/P = 0.8 and 1.0) increases the colloidal aggregate size to approximately 785 nm. The micelles are colloidally stable, which is not true for the PDPPS homopolymer at a similar molecular weight and the same B/P molar ratios (**Figure 7a**). The TEM image in **Figure 7e** confirms the existence of the micelles. Finally, the Lewis adduct-driven micellization is

partially reversible when triethylamine (TEA), which is a stronger Lewis base than phosphinostyrene, is added to the micelle solution (**Figure 7f**). On addition of TEA, the large colloidal aggregates disassemble, resulting in smaller micelles and free diblock copolymer. It is predicted that the TEA will preferentially bind to the BCF, breaking the B-P adduct and reversing the micellization process.

### **Outlook**

The three RIPT examples described within this Account demonstrate how chemical reactions such as polymerizations and adduct formation drive phase transitions, leading to changes in material structure. The final structure of the reported materials has been the focal point, but the fact that the mechanism driving structure formation in all three examples is a chemical reaction infers that the systems are kinetically controllable. Therefore, to push the RIPT field further, the fundamentals regarding chemical kinetics with respect to rates of reactions need to be applied to the formation of structure. There are only a few examples in which the polymerization rate and time scale associated with block copolymer self-assembly are addressed. Specifically, Hashimoto and coworkers explored polymerization-reaction-induced molecular self-assembly during living anionic polymerization and concluded that both polymerization rates and nanostructural self-assembly time scales need to be considered when controlling material structure during a reaction. Combining reaction kinetics with morphology transitions is multifaceted, and incorporating the time domain into RIPT is expected to enable new ways to dictate material structure, leading to materials discovery via polymerization pathway- and rate-dependent morphologies.

As demonstrated in equilibrium block copolymer self-assembly examples over the decades, the combination of experiment and theory is critical in uncovering fundamental self-

assembly processes. Similar synergies are necessary to uncover how kinetically controlled

structures result in either equilibrium or non-equilibrium states. The first issue to resolve is

differentiating between the two states, which includes establishing what is the expected

equilibrium state using theory and simulations. If a system is out of equilibrium, the next step is to

quantify the degree that a system is non-equilibrium. The "difference" between non-dissipative

and equilibrium states would include either quantifying an activation energy barrier or time

necessary to reach the lowest energy state. Finally, revealing the mechanism of the

chemical/structural transition will open new opportunities for tailoring final structures not possible

using equilibrium concepts.

**Author Information** 

**Corresponding Author** 

Robert J. Hickey – Department of Materials Science and Engineering, and Materials Research

Institute, The Pennsylvania State University, University Park, Pennsylvania, 16802, United States

ORCID: 0000-0001-6808-7411

E-mail: rjh64@psu.edu

Notes

The author declares no competing financial interests.

28

# **Biography**

Prof. Robert J. Hickey is currently an Associate Professor in the Department of Materials Science and Engineering at The Pennsylvania State University. He received his B.S. and Ph.D. in Chemistry at Widener University (2007) and the University of Pennsylvania (2013), respectively. He conducted his postdoctoral research at the University of Minnesota (2013 – 2016) and started his independent career at The Pennsylvania State University in 2016. The Hickey group investigates kinetic and non-equilibrium chemical and self-assembly methods to create hierarchically ordered polymeric materials.

# Acknowledgments

The work highlighted in this Account was supported by the National Science Foundation (CAREER Award DMR-1942508 & CHE-2203675) and the Air Force Office of Scientific Research (Young Investigator Prize 18RT0680).

#### References

- (1) Muthukumar, M.; Ober, C. K.; Thomas, E. L. Competing Interactions and Levels of Ordering in Self-Organizing Polymeric Materials. *Science* **1997**, *277*, 1225-1232.
- (2) Bates, F. S.; Hillmyer, M. A.; Lodge, T. P.; Bates, C. M.; Delaney, K. T.; Fredrickson, G. H. Multiblock Polymers: Panacea or Pandora's Box? *Science* **2012**, *336*, 434-440.
- (3) Bates, C. M.; Bates, F. S. 50th Anniversary Perspective: Block Polymers—Pure Potential. *Macromolecules* **2017**, *50*, 3-22.
- (4) Matyjaszewski, K. Atom Transfer Radical Polymerization (ATRP): Current Status and Future Perspectives. *Macromolecules* **2012**, *45*, 4015-4039.

- (5) Foerster, S.; Khandpur, A. K.; Zhao, J.; Bates, F. S.; Hamley, I. W.; Ryan, A. J.; Bras, W. Complex Phase Behavior of Polyisoprene-Polystyrene Diblock Copolymers Near the Order-Disorder Transition. *Macromolecules* **1994**, *27*, 6922-6935.
- (6) Leibler, L. Theory of Microphase Separation in Block Copolymers. *Macromolecules* **1980**, *13*, 1602-1617.
- (7) Fredrickson, G. H.; Helfand, E. Fluctuation Effects in the Theory of Microphase Separation in Block Copolymers. *J. Chem. Phys.* **1987**, *87*, 697-705.
- (8) Matsen, M. W. The Standard Gaussian Model for Block Copolymer Melts. *J. Phys. Condens. Matter* **2002**, *14*, R21.
- (9) Chanpuriya, S.; Kim, K.; Zhang, J.; Lee, S.; Arora, A.; Dorfman, K. D.; Delaney, K. T.; Fredrickson, G. H.; Bates, F. S. Cornucopia of Nanoscale Ordered Phases in Sphere-Forming Tetrablock Terpolymers. *ACS Nano* **2016**, *10*, 4961-4972.
- (10) Canning, S. L.; Smith, G. N.; Armes, S. P. A Critical Appraisal of RAFT-Mediated Polymerization-Induced Self-Assembly. *Macromolecules* **2016**, *49*, 1985-2001.
- (11) Seo, M.; Hillmyer, M. A. Reticulated Nanoporous Polymers by Controlled Polymerization-Induced Microphase Separation. *Science* **2012**, *336*, 1422-1425.
- (12) Lequieu, J.; Magenau, A. J. D. Reaction-Induced Phase Transitions with Block Copolymers in Solution and Bulk. *Polym. Chem.* **2021**, *12*, 12-28.
- (13) Inoue, T. Reaction-Induced Phase Decomposition in Polymer Blends. *Prog. Polym. Sci.* **1995**, *20*, 119-153.
- (14) Leguizamon, S. C.; Powers, J.; Ahn, J.; Dickens, S.; Lee, S.; Jones, B. H. Polymerization-Induced Phase Separation in Rubber-Toughened Amine-Cured Epoxy Resins: Tuning Morphology from the Nano- to Macro-scale. *Macromolecules* **2021**, *54*, 7796-7807.
- (15) *Modern Styrenic Polymers: Polystrenes and Styrenic Copolymers*; Scheirs, J.; Priddy, D., Eds.; John Wiley & Sons Ltd: West Sussex, England, 2003.
- (16) Schulze, M. W.; McIntosh, L. D.; Hillmyer, M. A.; Lodge, T. P. High-Modulus, High-Conductivity Nanostructured Polymer Electrolyte Membranes via Polymerization-Induced Phase Separation. *Nano Lett.* **2014**, *14*, 122-126.
- (17) Penfold, N. J. W.; Yeow, J.; Boyer, C.; Armes, S. P. Emerging Trends in Polymerization-Induced Self-Assembly. *ACS Macro Lett.* **2019**, *8*, 1029-1054.
- (18) Li, Y.; Armes, S. P. RAFT Synthesis of Sterically Stabilized Methacrylic Nanolatexes and Vesicles by Aqueous Dispersion Polymerization. *Angew. Chem. Int. Ed.* **2010**, *49*, 4042-4046.
- (19) Seo, M.; Kim, S.; Oh, J.; Kim, S.-J.; Hillmyer, M. A. Hierarchically Porous Polymers from Hyper-cross-linked Block Polymer Precursors. *J. Am. Chem. Soc.* **2015**, *137*, 600-603.
- (20) Shin, Y.; Brangwynne, C. P. Liquid Phase Condensation in Cell Physiology and Disease. *Science* **2017**, *357*, eaaf4382.
- (21) Howe, D. H.; Hart, J. L.; McDaniel, R. M.; Taheri, M. L.; Magenau, A. J. D. Functionalization-Induced Self-Assembly of Block Copolymers for Nanoparticle Synthesis. *ACS Macro Lett.* **2018**, *7*, 1503-1508.
- (22) Wei, Y.; Cui, S.; Yu, L.; Ding, J. Degradation-Influenced/Induced Self-Assembly of Copolymers with the Combinatory Effects of Changed Molecular Weight and Dispersity. *Macromolecules* **2023**, *56*, 2619-2636.
- (23) Hilaire, T.; Xu, Y.; Mei, W.; Riggleman, R. A.; Hickey, R. J. Lewis Adduct-Induced Phase Transitions in Polymer/Solvent Mixtures. *ACS Polym. Au* **2022**, *2*, 35–41.
- (24) Grzybowski, B. A.; Fitzner, K.; Paczesny, J.; Granick, S. From Dynamic Self-Assembly to Networked Chemical Systems. *Chem. Soc. Rev.* **2017**, *46*, 5647-5678.

- (25) Sorrenti, A.; Leira-Iglesias, J.; Markvoort, A. J.; de Greef, T. F. A.; Hermans, T. M. Non-Equilibrium Supramolecular Polymerization. *Chem. Soc. Rev.* **2017**, *46*, 5476-5490.
- (26) Chandran, S.; Baschnagel, J.; Cangialosi, D.; Fukao, K.; Glynos, E.; Janssen, L. M. C.; Müller, M.; Muthukumar, M.; Steiner, U.; Xu, J.; Napolitano, S.; Reiter, G. Processing Pathways Decide Polymer Properties at the Molecular Level. *Macromolecules* **2019**, *52*, 7146-7156.
- (27) Müller, M.; Abetz, V. Nonequilibrium Processes in Polymer Membrane Formation: Theory and Experiment. *Chem. Rev.* **2021**, *121*, 14189-14231.
- (28) Kimata, S.; Sakurai, T.; Nozue, Y.; Kasahara, T.; Yamaguchi, N.; Karino, T.; Shibayama, M.; Kornfield, J. A. Molecular Basis of the Shish-Kebab Morphology in Polymer Crystallization. *Science* **2007**, *316*, 1014-1017.
- (29) Sai, H.; Tan, K. W.; Hur, K.; Asenath-Smith, E.; Hovden, R.; Jiang, Y.; Riccio, M.; Muller, D. A.; Elser, V.; Estroff, L. A.; Gruner, S. M.; Wiesner, U. Hierarchical Porous Polymer Scaffolds from Block Copolymers. *Science* **2013**, *341*, 530-534.
- (30) Lang, C.; LaNasa, J. A.; Utomo, N.; Xu, Y.; Nelson, M. J.; Song, W.; Hickner, M. A.; Colby, R. H.; Kumar, M.; Hickey, R. J. Solvent-Non-Solvent Rapid-Injection for Preparing Nanostructured Materials from Micelles to Hydrogels. *Nat. Commun.* **2019**, *10*, 3855.
- (31) Ahn, N. Y.; Kwon, S.; Cho, S.; Kang, C.; Jeon, J.; Lee, W. B.; Lee, E.; Kim, Y.; Seo, M. In Situ Supramolecular Polymerization of Micellar Nanoobjects Induced by Polymerization. *ACS Macro Lett.* **2022**, *11*, 149-155.
- (32) Zofchak, E. S.; LaNasa, J. A.; Mei, W.; Hickey, R. J. Polymerization-Induced Nanostructural Transitions Driven by In Situ Polymer Grafting. *ACS Macro Lett.* **2018**, *7*, 822-827.
- (33) Zofchak, E. S.; LaNasa, J. A.; Torres, V. M.; Hickey, R. J. Deciphering the Complex Phase Behavior during Polymerization-Induced Nanostructural Transitions of a Block Polymer/Monomer Blend. *Macromolecules* **2020**, *53*, 835-843.
- (34) Torres, V. M.; LaNasa, J. A.; Vogt, B. D.; Hickey, R. J. Controlling Nanostructure and Mechanical Properties in Triblock Copolymer/Monomer Blends via Reaction-Induced Phase Transitions. *Soft Matter* **2021**, *17*, 1505-1512.
- (35) Matsen, M. W. Cylinder Gyroid Epitaxial Transitions in Complex Polymeric Liquids. *Phys. Rev. Lett.* **1998**, *80*, 4470-4473.
- (36) Honda, T.; Kawakatsu, T. Epitaxial Transition from Gyroid to Cylinder in a Diblock Copolymer Melt. *Macromolecules* **2006**, *39*, 2340-2349.
- (37) Floudas, G.; Ulrich, R.; Wiesner, U.; Chu, B. Nucleation and Growth in Order-to-Order Transitions of a Block Copolymer. *Europhys. Lett.* **2000**, *50*, 182.
- (38) Hajduk, D. A.; Takenouchi, H.; Hillmyer, M. A.; Bates, F. S.; Vigild, M. E.; Almdal, K. Stability of the Perforated Layer (PL) Phase in Diblock Copolymer Melts. *Macromolecules* **1997**, *30*, 3788-3795.
- (39) Vukovic, I.; ten Brinke, G.; Loos, K. Hexagonally Perforated Layer Morphology in PS-b-P4VP(PDP) Supramolecules. *Macromolecules* **2012**, *45*, 9409-9418.
- (40) Matsen, M. W. Effect of Architecture on the Phase Behavior of AB-Type Block Copolymer Melts. *Macromolecules* **2012**, *45*, 2161-2165.
- (41) Zhu, Y.; Burgaz, E.; Gido, S. P.; Staudinger, U.; Weidisch, R.; Uhrig, D.; Mays, J. W. Morphology and Tensile Properties of Multigraft Copolymers with Regularly Spaced Tri-, Tetra-, and Hexafunctional Junction Points. *Macromolecules* **2006**, *39*, 4428-4436.
- (42) Kumar, S. K.; Benicewicz, B. C.; Vaia, R. A.; Winey, K. I. 50th Anniversary Perspective: Are Polymer Nanocomposites Practical for Applications? *Macromolecules* **2017**, *50*, 714-731.

- (43) Kumar, S. K.; Ganesan, V.; Riggleman, R. A. Perspective: Outstanding Theoretical Questions in Polymer-Nanoparticle Hybrids. *J. Chem. Phys.* **2017**, *147*, 020901.
- (44) Kojima, Y.; Usuki, A.; Kawasumi, M.; Okada, A.; Fukushima, Y.; Kurauchi, T.; Kamigaito, O. Mechanical Properties of Nylon 6-Clay Hybrid. *J. Mater. Res.* **1993**, *8*, 1185-1189.
- (45) Usuki, A.; Kojima, Y.; Kawasumi, M.; Okada, A.; Fukushima, Y.; Kurauchi, T.; Kamigaito, O. Synthesis of Nylon 6-Clay Hybrid. *J. Mater. Res.* **1993**, *8*, 1179-1184.
- (46) Demir, M. M.; Castignolles, P.; Akbey, Ü.; Wegner, G. In-Situ Bulk Polymerization of Dilute Particle/MMA Dispersions. *Macromolecules* **2007**, *40*, 4190-4198.
- (47) Dean, L. M.; Ravindra, A.; Guo, A. X.; Yourdkhani, M.; Sottos, N. R. Photothermal Initiation of Frontal Polymerization Using Carbon Nanoparticles. *ACS Appl. Polym. Mater.* **2020**, *2*, 4690-4696.
- (48) Hou, D.; Bostwick, J. E.; Shallenberger, J. R.; Zofchak, E. S.; Colby, R. H.; Liu, Q.; Hickey, R. J. Simultaneous Reduction and Polymerization of Graphene Oxide/Styrene Mixtures to Create Polymer Nanocomposites with Tunable Dielectric Constants. *ACS Appl. Nano Mater.* **2020**, *3*, 962-968.
- (49) LaNasa, J. A.; Torres, V. M.; Hickey, R. J. In Situ Polymerization and Polymer Grafting to Stabilize Polymer-Functionalized Nanoparticles in Polymer Matrices. *J. Appl. Phys.* **2020**, *127*, 134701.
- (50) Sevening, J. N.; Dottin, S.; Torres, V. M.; Hickey, R. J. Soft Hybrid Elastomers Containing Polymer Grafted Nanoparticles. *Giant* **2022**, *12*, 100133.
- (51) LaNasa, J. A.; Neuman, A.; Riggleman, R. A.; Hickey, R. J. Investigating Nanoparticle Organization in Polymer Matrices during Reaction-Induced Phase Transitions and Material Processing. *ACS Appl. Mater. Interfaces* **2021**, *13*, 42104-42113.
- (52) LaNasa, J. A.; Hickey, R. J. Surface-Initiated Ring-Opening Metathesis Polymerization: A Method for Synthesizing Polymer-Functionalized Nanoparticles Exhibiting Semicrystalline Properties and Diverse Macromolecular Architectures. *Macromolecules* **2020**, *53*, 8216-8232.
- (53) Molau, G. E.; Keskkula, H. Heterogeneous Polymer Systems. IV. Mechanism of Rubber Particle Formation in Rubber-Modified Vinyl Polymers. *J. Polym. Sci., Part A: Polym. Chem.* **1966**, *4*, 1595-1607.
- (54) Kumar, S. K.; Jouault, N.; Benicewicz, B.; Neely, T. Nanocomposites with Polymer Grafted Nanoparticles. *Macromolecules* **2013**, *46*, 3199-3214.
- (55) Peng, S.; Lee, Y.; Wang, C.; Yin, H.; Dai, S.; Sun, S. A Facile Synthesis of Monodisperse Au Nanoparticles and their Catalysis of CO Oxidation. *Nano Res.* **2008**, *1*, 229-234.
- (56) Sing, C. E.; Perry, S. L. Recent Progress in the Science of Complex Coacervation. *Soft Matter* **2020**, *16*, 2885-2914.
- (57) Li, P.; Banjade, S.; Cheng, H.-C.; Kim, S.; Chen, B.; Guo, L.; Llaguno, M.; Hollingsworth, J. V.; King, D. S.; Banani, S. F.; Russo, P. S.; Jiang, Q.-X.; Nixon, B. T.; Rosen, M. K. Phase Transitions in the Assembly of multivalent Signalling Proteins. *Nature* **2012**, *483*, 336-340.
- (58) Lunde, B. M.; Moore, C.; Varani, G. RNA-Binding Proteins: Modular Design for Efficient Function. *Nat. Rev. Mol. Cell Biol.* **2007**, *8*, 479-490.
- (59) Yamauchi, K.; Hasegawa, H.; Hashimoto, T.; Tanaka, H.; Motokawa, R.; Koizumi, S. Direct Observation of Polymerization-Reaction-Induced Molecular Self-Assembling Process: In-Situ and Real-Time SANS Measurements during Living Anionic Polymerization of Polyisoprene-block-Polystyrene. *Macromolecules* **2006**, *39*, 4531-4539.

(60) Iida, Y.; Kawakatsu, T.; Motokawa, R.; Koizumi, S.; Hashimoto, T. Transition in Domain Morphology of Block Copolymers Undergoing Polymerization. *Macromolecules* **2008**, *41*, 9722-9726.